


De novo biosynthesis of garbanzol and fustin in *Streptomyces albus* based on a potential flavanone 3-hydroxylase with 2-hydroxylase side activity

Laura Marín,^{1,2,3,††} Ignacio Gutiérrez-del-Río,^{1,2,3,††}
Claudio Jesús Villar^{1,2,3} and Felipe Lombó^{1,2,3,*} 

¹Research Group BIONUC (Biotechnology of Nutraceuticals and Bioactive Compounds), Departamento de Biología Funcional, Área de Microbiología, Universidad de Oviedo, Oviedo, Principality of Asturias, Spain.

²IUOPA (Instituto Universitario de Oncología del Principado de Asturias), Oviedo, Principality of Asturias, Spain.

³ISPA (Instituto de Investigación Sanitaria del Principado de Asturias), Oviedo, Principality of Asturias, Spain.

Summary

Flavonoids are important plant secondary metabolites, which were shown to have antioxidant, anti-inflammatory or antiviral activities. Heterologous production of flavonoids in engineered microbial cell factories is an interesting alternative to their purification from plant material representing the natural source. The use of engineered bacteria allows to produce specific compounds, independent of soil, climatic or other plant-associated production parameters. The initial objective of this study was to achieve an engineered production of two interesting flavanones, garbanzol and fustin, using *Streptomyces albus* as the production host. Unexpectedly, the engineered strain produced several flavones and flavonols in the absence of the additional expression

of a flavone synthase (FNS) or flavonol synthase (FLS) gene. It turned out that the heterologous flavanone 3-hydroxylase (F3H) has a 2-hydroxylase side activity, which explains the observed production of 7,4'-dihydroxyflavone, resokaempferol, kaempferol and apigenin, as well as the biosynthesis of the extremely rare 2-hydroxylated intermediates 2-hydroxyliquiritigenin, 2-hydroxynaringenin and probably licodione. Other related metabolites, such as quercetin, dihydroquercetin and eriodictyol, have also been detected in culture extracts of this recombinant strain. Hence, the enzymatic versatility of *S. albus* can be conveniently exploited for the heterologous production of a large diversity of plant metabolites of the flavonoid family.

Introduction

Flavonoids comprise a large family of polyphenols, representing about 9,000 compounds ubiquitously distributed in plants (Kumar and Pandey, 2013; Li *et al.*, 2014; Shah *et al.*, 2019). They are one of the largest families of natural products and share a generic chemical structure consisting of 15 carbon atoms (C6-C3-C6). The core structure harbours two aromatic rings (rings A and B) connected by a heterocyclic tetrahydropyran (ring C) (Verma and Pratap, 2010; Ravishankar *et al.*, 2013; Yao *et al.*, 2014), and this molecule's backbone can carry multiple substituents, such as hydroxyl or methyl groups, as well as sugars (Crozier *et al.*, 2009). Flavonoids have received significant attention due to their medicinal value as nutraceuticals and cancer chemopreventive agents, acting against different types of chronic diseases related to the cardiovascular system (Sánchez *et al.*, 2019) or cancer (Fernández *et al.*, 2016; George *et al.*, 2017; Redondo-Blanco *et al.*, 2017). Recently, the flavonoid herbacetin was shown to inhibit 3C-like protease (3CLpro) of coronaviruses (CoVs) (Jo *et al.*, 2020). Outside of the field of medicine, flavonoids find potential applications in food preservation (Gutiérrez-del-Río *et al.*, 2018).

Similar to other flavonoids, fustin (sometimes called dihydrofisetin) and garbanzol are valuable nutraceuticals and have been found to possess antioxidant (Chen *et al.*, 2017), anticancer (Park *et al.*, 2004; Fotso *et al.*, 2017),

Received 2 February, 2021; revised 7 June, 2021; accepted 10 June, 2021.

For correspondence: *E-mail lombofelipe@uniovi.es; Tel. +34-98510-3593.

††These authors contributed equally to this work.

Microbial Biotechnology (2021) 14(5), 2009–2024
doi:10.1111/1751-7915.13874

Funding information

The University of Oviedo thanks Programa de Ayudas a Grupos de Investigación del Principado de Asturias (IDI/2018/000120), Programa Severo Ochoa de Ayudas Predoctorales para la investigación y docencia from Principado de Asturias (grant BP16023 to I.G.R.), Proyectos I + D+I, del Programa Estatal de Investigación, Desarrollo e Innovación Orientada a los Retos de la Sociedad, from Ministerio de Ciencia, Innovación y Universidades of Spain (AGL2017-88095-R) and the European Union's Horizon 2020 Research and Innovation Programme under Grant Agreement no. 814650 for the project SynBio4Flav.

© 2021 The Authors. *Microbial Biotechnology* published by Society for Applied Microbiology and John Wiley & Sons Ltd.

This is an open access article under the terms of the Creative Commons Attribution-NonCommercial-NoDerivs License, which permits use and distribution in any medium, provided the original work is properly cited, the use is non-commercial and no modifications or adaptations are made.

antibacterial (Jang *et al.*, 2018), antiviral (Kang *et al.*, 2012), anti-inflammatory (Li *et al.*, 2018) and neuroprotective (Park *et al.*, 2007) properties. Nevertheless, very little is known about the biological activities of licodione or 2-hydroxyliquiritigenin, and only two licodione derivatives (2'-methoxy-3'-prenyl-licodione and 2'-methoxy-3',3''-diprenyl-licodione) have been shown to possess isoprenylcysteine carboxyl methyltransferase (Icmt) inhibitory activity, proving their potential as anticancer agents (Buchanan *et al.*, 2008). The compound 7,4'-dihydroxyflavone was demonstrated to be a potent aromatase inhibitor (Pelissero *et al.*, 1996; Ta and Walle, 2007) and additionally inhibits expression of mucin 5AC (MUC5AC), a key mucin in obstructive lung disease (Liu *et al.*, 2015). Resokaempferol is known to have antitumor as well as anti-inflammatory properties and acts by blocking the activation of the JAK/STAT3 pathway by both LPS and IL-6 signalling (Lee *et al.*, 2010; Yu *et al.*, 2016).

In plants, the initial steps of flavonoid biosynthesis are part of the phenylpropanoid pathway, in which L-phenylalanine is converted to *p*-coumaroyl-CoA in three enzymatic steps, which are catalysed by phenylalanine ammonia-lyase (PAL, EC 4.3.1.24), cinnamate 4-hydroxylase (C4H, EC 1.14.14.91) and *p*-coumaroyl CoA ligase (4CL, EC 6.2.1.12; Falcone Ferreyra *et al.*, 2012; Chouhan *et al.*, 2017). However, in bacteria, the use of L-tyrosine as a substrate for tyrosine ammonia-lyase (TAL, EC 4.3.1.23) is preferred for heterologous biosynthesis purposes. L-tyrosine is already hydroxylated in the *para*-position of the aromatic ring, which circumvents the need for the additional hydroxylation step (that is catalysed by a plant-derived, membrane-bound cytochrome P450-dependent enzyme, cinnamate 4-hydroxylase, C4H enzyme; Kyndt *et al.*, 2002; Watts *et al.*, 2004; Fig. 1). Subsequently, chalcone synthase (CHS, EC 2.3.1.74) condenses a molecule of *p*-coumaroyl-CoA with three molecules of malonyl-CoA and circularizes the resulting polyketide to yield naringenin chalcone, which is then isomerized into naringenin by chalcone isomerase (CHI, EC 5.5.1.6). Naringenin is the common precursor for the biosynthesis of either dihydrokaempferol, kaempferol, apigenin, quercetin and eriodictyol (Fig. 1A), or liquiritigenin, for which an additional chalcone reductase (CHR, EC 2.3.1.170) is required (Fig. 1B). Liquiritigenin represents a central intermediate because biosynthetic pathways for garbanzol, fustin and resokaempferol as well as for licodione and 7,4'-dihydroxyflavone branch off at the stage of this compound. In order to synthesize garbanzol from liquiritigenin, the action of a flavanone 3-hydroxylase (F3H, EC 1.14.11.9) is required; then, the flavonoid 3'-hydroxylase (F3'H, EC 1.14.14.82) transforms garbanzol into fustin (Tsao, 2010; Wang *et al.*,

2011; Falcone Ferreyra *et al.*, 2012; Chouhan *et al.*, 2017).

The high market value of flavonoids makes them a very attractive target for mass production; in fact, based on the latest report on the market profitability of flavonoids, their total market value may reach 1.05 billion US dollars in 2021 (Shah *et al.*, 2019). Even though plants are the natural sources of flavonoids, the large-scale production of these compounds for further use as drugs remains a challenge. The amounts that can be obtained are limited, and extraction from plant material is unreliable due to unexpected seasonal changes. On the other hand, their chemical synthesis requires toxic chemicals and involves regioselective reactions that are difficult to control. Thus, an attractive alternative is to functionally introduce the plant biosynthetic pathways into microbial cell factories, which in this work is a member of the genus *Streptomyces* as the production host (Matkowski, 2008; Falcone Ferreyra *et al.*, 2012; Trantas *et al.*, 2015; Genilloud, 2017).

The engineered production of putative garbanzol has been previously achieved by combinatorial biosynthesis using *Escherichia coli* and *Saccharomyces cerevisiae* (Stahlhut *et al.*, 2015; Rodriguez *et al.*, 2017), but we report *de novo* biosynthesis of resokaempferol and garbanzol in *Streptomyces albus*. We also report *de novo* biosynthesis of fustin, 2-hydroxyliquiritigenin, licodione (tentative identification) and 7,4'-dihydroxyflavone in a microorganism. Additionally, we report for the very first time the biosynthesis of flavones and flavonols from flavanones and flavanonols, respectively, through 2-hydroxy intermediates and without the need for expression of an exogenous gene coding for an FNS or FLS. This fact suggests a possible catalytic F2H side activity of F3H, followed by an endogenous *S. albus* dehydratase activity; however, further studies are needed to unequivocally corroborate the assumption in this bacterium.

Results

Heterologous biosynthesis of garbanzol

The activity of six enzymes (TAL, 4CL, CHS, CHR, CHI and F3H) is required to produce garbanzol. In this work, six synthetic genes coding for the enzymes required for garbanzol biosynthesis (with codon usage adapted to the translation characteristics of *Streptomyces*) were cloned into a replicative high-copy number *E. coli*-*Streptomyces* shuttle vector under the control of P_{ermE}* (see Experimental Procedures section; Fig. 2A). The *ermE** promoter is one of the most widely used promoters for heterologous gene expression in streptomycetes (Lombó *et al.*, 2006; Park *et al.*, 2009; Wang *et al.*, 2012; Takano *et al.*, 2017; Liu *et al.*, 2018), and its correct activity for

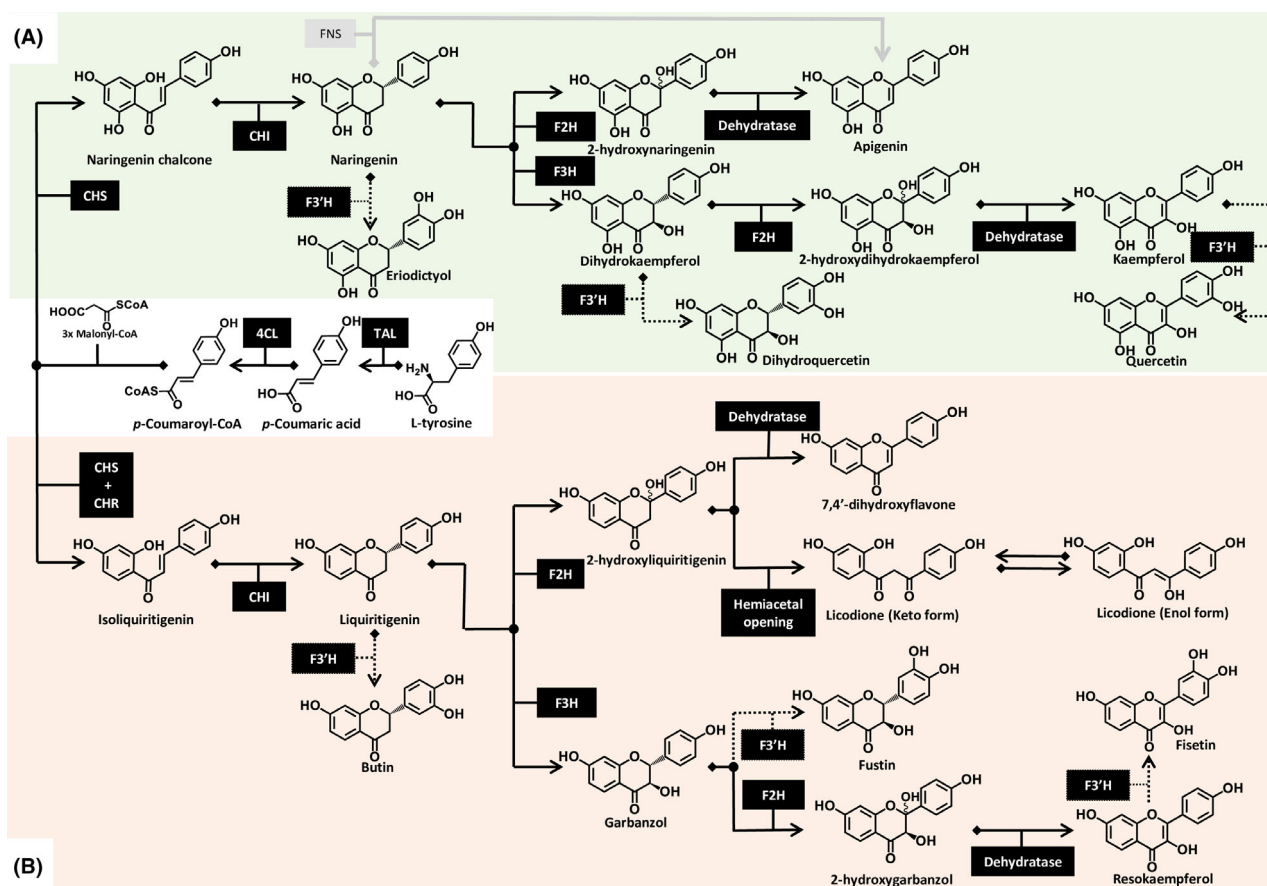


Fig. 1. Proposed biosynthetic pathway for *de novo* production of flavonoids and chalcone licodione from naringenin chalcone (A) and isoliquiritigenin (B). 4CL, *p*-coumarate CoA ligase; CHI, chalcone isomerase; CHR, chalcone reductase; CHS, chalcone synthase; F2H, flavanone 2-hydroxylase; F3'H, flavonoid 3'-hydroxylase; F3H, flavanone 3-hydroxylase; FNS, flavone synthase; TAL, tyrosine ammonia-lyase.

controlling flavonoid biosynthetic genes has been confirmed in previous studies of this research group (Marín *et al.*, 2017, 2018; García-Gutiérrez *et al.*, 2020). Genes were selected from different bacteria (*Rhodobacter capsulatus* and *S. coelicolor*) and plants (*Glycine max*, *Petroselinum crispum* and *Arabidopsis thaliana*) as they were already tested in the laboratory for these enzymatic steps (Marín *et al.*, 2017, 2018; García-Gutiérrez *et al.*, 2020). In bacteria, the use of TAL is preferred for heterologous biosynthesis purposes, as starting from L-tyrosine, the need for the C4H activity (a plant membrane-bound enzyme) does not longer exist. Because almost all the TALs show activity towards both phenylalanine and tyrosine, TAL enzyme from *R. capsulatus* was chosen based on its high affinity for tyrosine ($K_m = 160$), instead of phenylalanine ($K_m = 560$) (Xue *et al.*, 2007). The following enzymes 4CL, CHS, CHR and CHI, common to both garbanzol and fustin biosynthesis, were chosen from *S. coelicolor* and *Glycine max* as they were already functioning properly in other experiments (Marín *et al.*, 2017, 2018; García-Gutiérrez

et al., 2020). The final plasmid pGR was used for the transformation of *S. albus* J1074, yielding *S. albus* pGR. The recombinant strain was then tested for garbanzol production.

To confirm the heterologous production of garbanzol, the constructed strain *S. albus* pGR was cultivated, and extracts of the culture were analysed by HPLC-HRESIMS. Simultaneously, a negative control strain carrying the empty vector pAGO, *S. albus* pAGO, was analysed under the same conditions and compared with *S. albus* pGR. The obtained base peak chromatograms (BPCs) were extracted for the mass peak m/z 271.06118 $[M-H]^-$ (calculated for $C_{15}H_{12}O_5$), with a mass error range of 0.005 mmu (millimass units). The obtained extracted ion chromatograms (EICs) revealed the presence of six peaks (retention times: 4.7, 5.0, 5.1, 5.3, 6.5 and 6.7 min) for the proposed m/z that were all absent in the negative control *S. albus* pAGO (Fig. 3A). The retention time and the observed ions for two (peak 2 and peak 6, Fig. 3B) of the five detected peaks were consistent with those observed in the garbanzol and

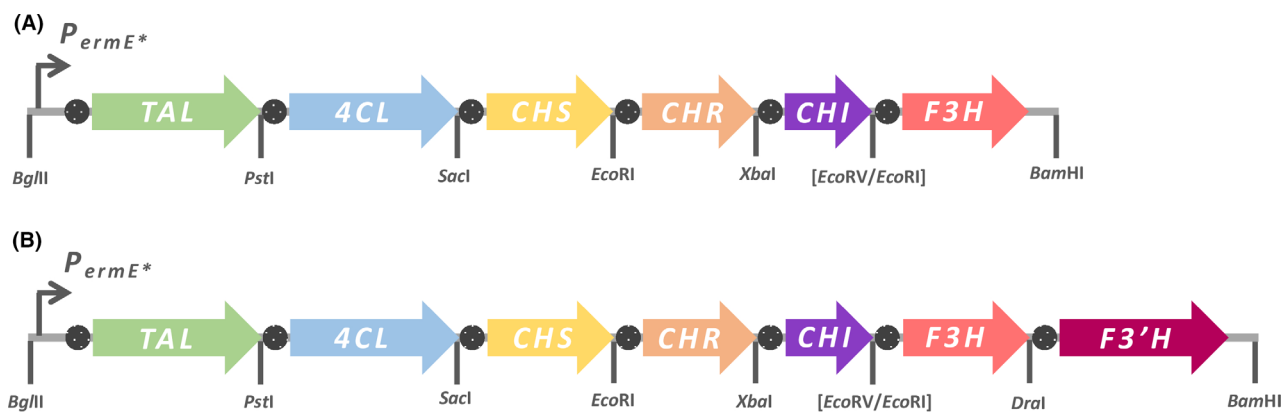


Fig. 2. Designed gene clusters for heterologous expression of garbanzol (A) and fustin (B) in *S. albus*. Both DNA constructions were finally subcloned as a *Bgl*II-*Bam*HI fragment into the pLAGO plasmid. Blocked restriction enzymes sites (after DNA polymerase I Klenow fragment treatment during subcloning) are represented in brackets.

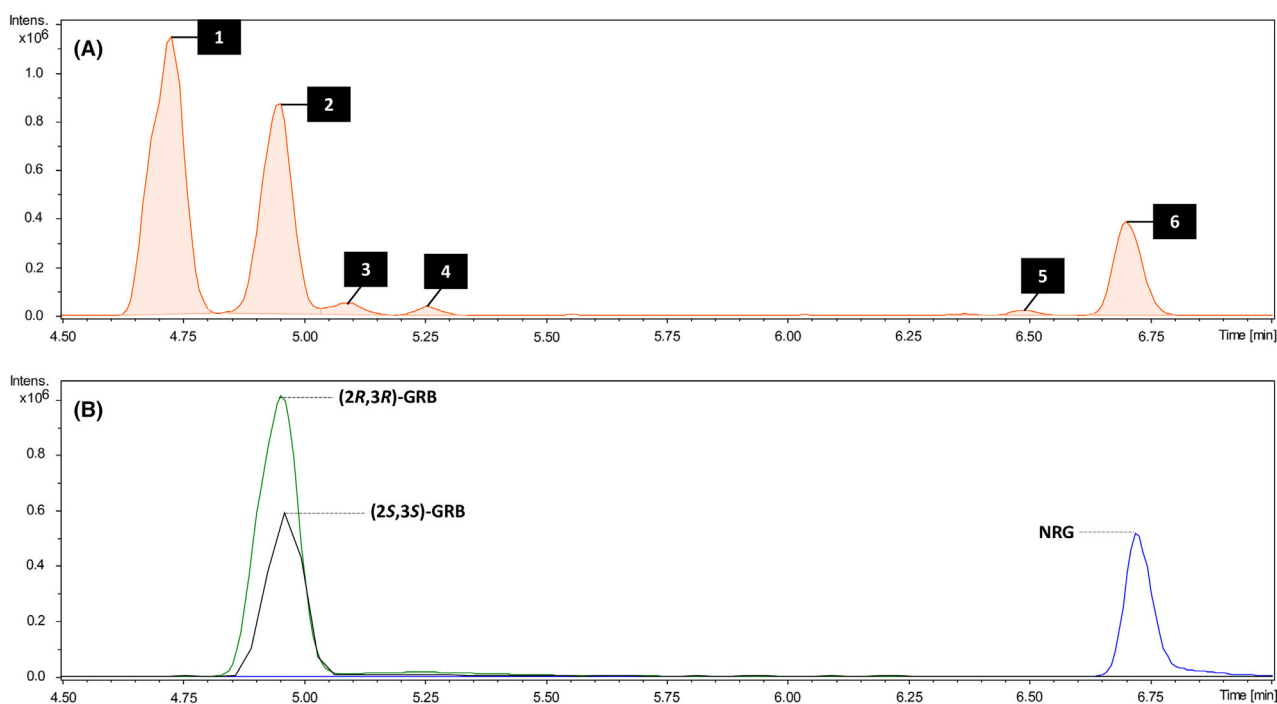


Fig. 3. EICs at m/z 271.06118 \pm 0.005 [M-H]⁻ of *S. albus* pGR and *S. albus* pDF crude extract (A) and commercial flavonoids standards of NRG (naringenin) and GRB (garbanzol) (B). Peak 1 corresponds to 2-hydroxyliquiritigenin (probably two isomers based on the stereochemistry of the 2-hydroxyl group), peak 2 corresponds to the two commercial garbanzol enantiomers, peaks 3 and 4 probably correspond to different tautomeric forms of licodione (tentative identification) and peak 6 corresponds to naringenin. GRB, garbanzol; NRG, naringenin.

naringenin commercial standards respectively. However, peaks 1, 3, 4 and 5 (Fig. 3A) could not be assigned to any of the flavonoids taking part in the proposed biosynthetic pathway; hence, further studies were carried out to identify those unknown compounds, focusing on peak 1.

A time-course cultivation of the garbanzol-producing strain *S. albus* pGR and the negative control strain *S. albus* pLAGO was carried out. In this experiment,

biomass concentrations and garbanzol titres were monitored over 168 h of incubation (Fig. 4), showing that the growth of the garbanzol-producing strain is similar to the control strain as no statistically significant differences were observed between both strain growth curve values, except for the biomass value at 72 h. Also, there are not statistically significant differences between the final dry cell weight at 168 h between both strains (Fig. 4). This

rules out a possible toxic effect of some of the pathway intermediates or the end-products associated with the cloned biosynthetic pathway. Garbanzol titres increased during the exponential phase (until 72 h in R5A medium), and a maximum was detected at the beginning of the stationary phase (96 h). Then, the garbanzol titres started to decline in the days following incubation (Fig. 4). Interestingly, this drop from the maximum production is accompanied by an increase in the relative intensity of peak 1 (see Section Identification of liquiritigenin derivatives: 2-hydroxyliquiritigenin, licodione and 7,4'-dihydroxyflavone produced by the *S. albus* pGR strain), the maximum of which was reached at 144–168 h. This fact led to the belief that there might be a biosynthetic relationship between garbanzol and peak 1 (Fig. S5).

A comparison between the culture supernatant and cellular pellet was carried out to detect the main flavonoid compounds, both after solvent extraction (Fig. S4). Interestingly, the compound distribution was not the expected one as in the culture supernatant, mostly, *p*-coumaric acid, garbanzol and 2-hydroxyliquiritigenin were present. However, naringenin was mainly present in cellular pellet extracts. Isoliquiritigenin and liquiritigenin were similarly distributed between both organic extracts. This could imply the presence of specific membrane transporters in *S. albus* for some of these nutraceutical polyphenols.

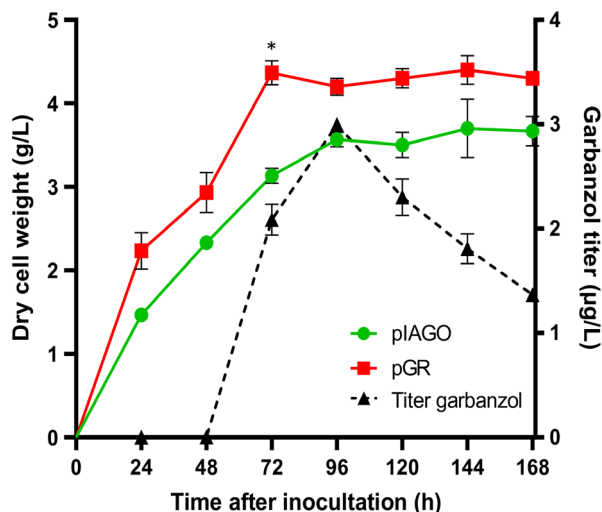


Fig. 4. Cultivation data (dry cell weight) of *S. albus* pGR (red) and negative control *S. albus* pIAGO (green) grown on R5A medium sampled every 24 h over 168 h. Garbanzol titres in $\mu\text{g l}^{-1}$ have been overlaid (dashed line). The data are expressed as mean value \pm standard error of mean (SEM). * indicate statistically significant differences between both strains (*S. albus* pGR and negative control *S. albus* pIAGO) after two-way ANOVA.

Identification of liquiritigenin derivatives: 2-hydroxyliquiritigenin, licodione and 7,4'-dihydroxyflavone produced by the *S. albus* pGR strain

With the objective of deciphering the identity of the most abundant isomers of garbanzol under negative ionization conditions (peak 1), the engineered *S. albus* pGR strain was regrown (6 l laboratory scale) and submitted to HRESIMS-guided fractionation with different consecutive fractionation steps (SPE fractionation and semipreparative HPLC fractionation; see Section Experimental procedures). After purification, 0.8 mg of an almost pure compound was obtained, and the putative elucidation of the structure was performed on the basis of HPLC-HRESIMS/MS, LC-UV/vis and 1D-2D-NMR methods using the analysis of MS-, MS²-, UV/vis absorbance-, COSY- and HSQC-generated spectra. An authentic standard of (2*R*,3*R*)-garbanzol was also submitted to the same spectrometric and spectroscopic analyses, and all spectra were added to the pool of data available in our research group for commercially available flavonoids.

The MS spectrum for this new molecule showed a deprotonated ion at m/z 271.0613 [M-H]⁻, consistent with the molecular formula C₁₅H₁₂O₅ (calculated m/z 271.06118 [M-H]⁻). Examination of UV/vis and MS² datasets led to similar absorbance peaks (Fig. 5) and identical fragmentation patterns compared with authentic commercial garbanzol (Fig. 6A), revealing the existence of a putative isomer of garbanzol. Although the chromatographic analysis showed a major peak with minor contaminants, the NMR analysis failed because no major signals arose and a vast mixture of minor compounds was detected. Interestingly, the HSQC spectrum did not show any oxygenated methine carbon. This fact not only excluded this new molecule to be a stereoisomer of garbanzol but also indicated the presence of a potential hydroxylation in the C2 position of the C ring, which would in fact correspond to 2-hydroxyliquiritigenin. However, stronger evidence about a positional isomer differing in the location of the hydroxyl group was needed to validate this hypothesis. Additionally, commercial (2*S*,3*S*)-garbanzol, which is a naturally occurring enantiomer of the (2*R*,3*R*)-garbanzol produced in the present study (Hashida *et al.*, 2014), was purchased, but it showed an identical retention time as (2*R*,3*R*)-garbanzol (Fig. 3B). To gain an insight into this proposed C2 hydroxylation, the HPLC-HRESIMS/MS fragmentation profile of the new molecule, possibly 2-hydroxyliquiritigenin, was studied (Fig. 6B and C, see Appendix S1). The presence of a shoulder peak on the left side of peak 1 could point to the existence of two stereoisomers in relation to the position of the 2-hydroxy moiety at C2 of the heterocycle (Fig. 3A).

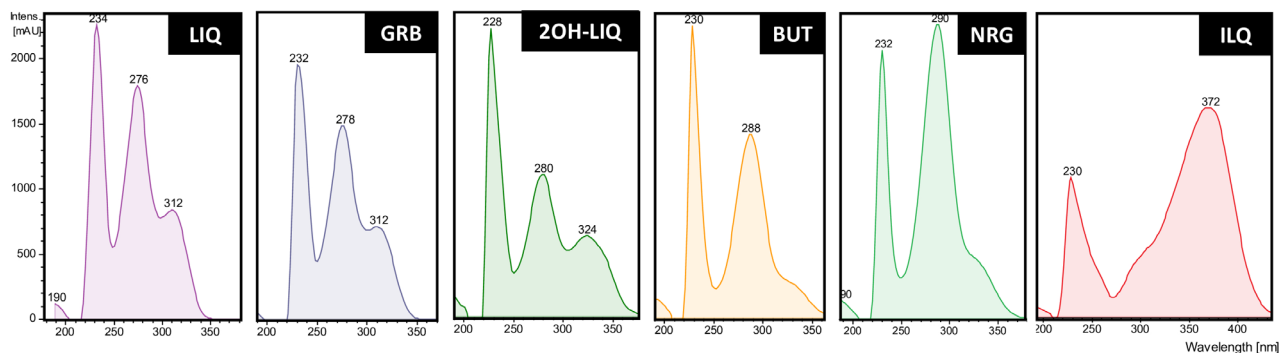


Fig. 5. UV/vis spectra of several commercial flavonoid standards and purified putative 2-hydroxyliquiritigenin with m/z 271.0613 $[M-H]^-$ (peak 1 in Fig. 3A). 2OH-LIQ, 2-hydroxyliquiritigenin; BUT, butin; ILQ, isoliquiritigenin; LIQ, liquiritigenin; NRG, naringenin.

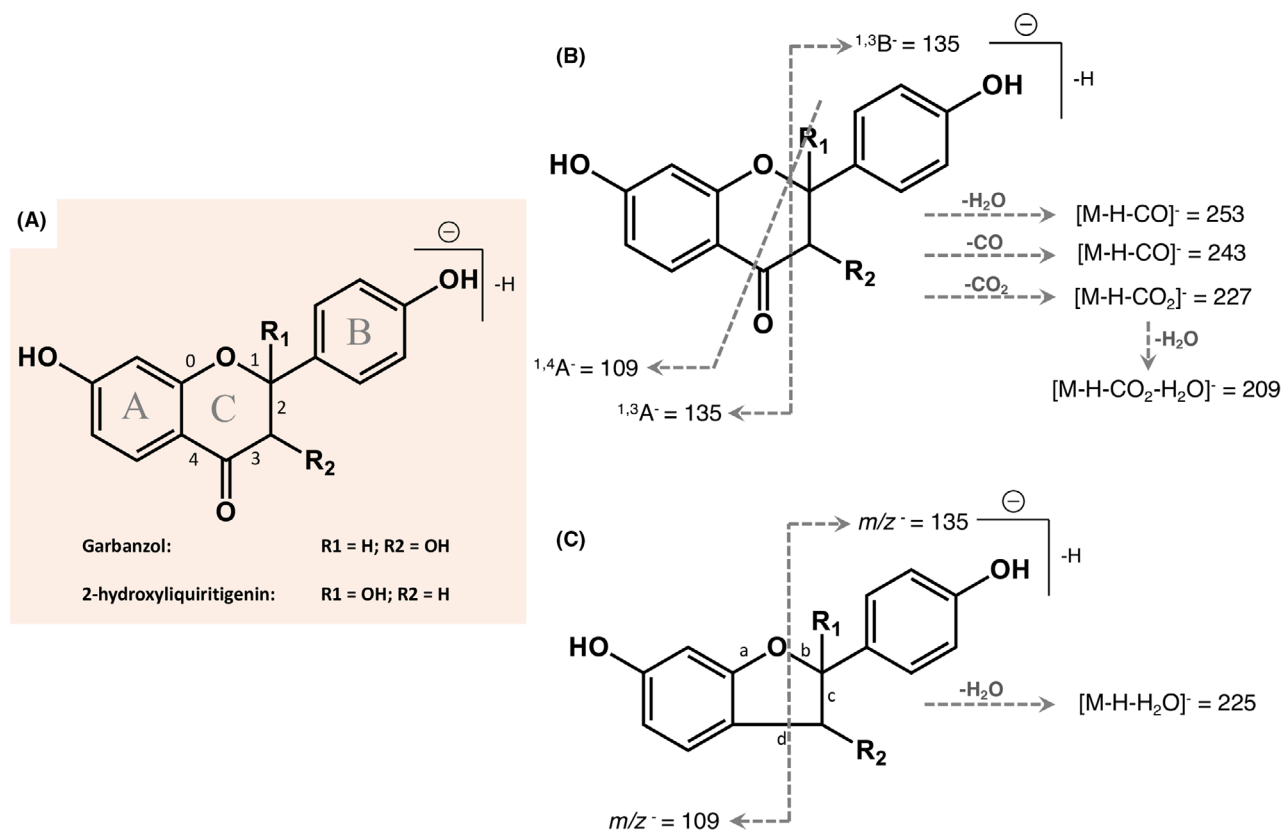


Fig. 6. HPLC-HRESIMS/MS analysis of authentic garbanzol and purified 2-hydroxyliquiritigenin. According to the nomenclature of Yang *et al.* each fragment is denoted by the combined use of $^{14}A^-$ or $^{14}B^-$. A and B represent the flavonoid intact ring, and the superscript on the left indicates the broken bounds of the deprotonated molecule (Yang *et al.*, 2012). A, Proposed retrocyclization cleavages of the C ring. B, MS^2 fragmentation products for the parent ion m/z 271.0535 $[M-H]^-$. C, MS^2 fragmentation products for the in-source-formed species m/z 243.0591 $[M-H]^-$. Product ions resulting from losses of H_2O , CO and CO_2 have also been included.

To confirm the existence of an alternative biosynthetic pathway leading to licodione/7,4'-dihydroxyflavone, the BPC obtained from the crude organic extraction of *S. albus* pGR was re-analysed in detail for the presence of ions corresponding to licodione (calculated m/z 271.06118 $[M-H]^-$; $C_{15}H_{12}O_5$) and 7,4'-dihydroxyflavone

(calculated m/z 253.05062 $[M-H]^-$; $C_{15}H_{10}O_4$). The EIC for the mass peak 271.06118 $[M-H]^-$ showed the six peaks previously described (peaks 1–6) (Fig. 3A), with three of them representing known compounds: garbanzol (peak 2), 2-hydroxyliquiritigenin (peak 1, tentative identification) and naringenin (peak 6). The unidentified peaks

3, 4 and 5 could belong to different tautomeric forms of licodione (keto- and enol forms). When the m/z 253.05062 $[M-H]^-$ ion was extracted, an unknown peak in the chromatogram at 5.5 min was observed (Fig. S2B). For both EICs, a mass error range of 0.005 mmu was selected, and they were not present in the negative control *S. albus* pLAGO (data not shown). The presence of both compounds could be confirmed using authentic licodione (keto form) and 7,4'-dihydroxyflavone standards, but only the latter was commercially available and could be analysed under HPLC-HRESIMS conditions. The standard proved the presence of 7,4'-dihydroxyflavone (Fig. S2B) in the recombinant strain *S. albus* pGR constructed in this work. Thus, the existence of this molecule confirmed the presence of an unexpected additional pathway that generates 7,4'-dihydroxyflavone from liquiritigenin with 2-hydroxyliquiritigenin as potential intermediate (Fig. 1B).

Identification of the flavanone dihydrokaempferol and other flavone and flavonol derivatives: apigenin, resokaempferol and kaempferol produced by the S. albus pGR strain

The crude organic extract of *S. albus* pGR and the different SPE (solid-phase extraction) fractions (I to VI) obtained during the purification process of 2-hydroxyliquiritigenin were screened using HPLC-HRESIMS for the presence of flavonoids, for which MS data was available. Interestingly, clear signals of the deprotonated molecule mass peaks at m/z 269.0467/269.0457 $[M-H]^-$ (two signals with different retention times), m/z 287.0563 $[M-H]^-$ and m/z 285.0402 $[M-H]^-$ were detected which eluted at the same retention time and were consistent with apigenin (calculated m/z 269.04553 $[M-H]^-$; $C_{15}H_{10}O_5$), resokaempferol (calculated m/z 269.04553 $[M-H]^-$; $C_{15}H_{12}O_5$), dihydrokaempferol (calculated m/z 287.05610 $[M-H]^-$; $C_{15}H_{12}O_6$) and kaempferol (calculated m/z 285.04045 $[M-H]^-$; $C_{15}H_{10}O_6$) respectively (Fig. S2B). Besides, the EIC at m/z 287.05610 $[M-H]^-$ showed one additional distinct peak (m/z 287.0569 $[M-H]^-$) at a different retention time, which belongs to a molecule with the proposed molecular formula $C_{15}H_{12}O_6$. In addition to dihydrokaempferol, the identified peak corresponds to 2-hydroxynaringenin, a coelutant of the commercial 2-hydroxynaringenin standard (Fig. S2B). In relation to this 2-hydroxy-derivative, a residual signal at m/z 303.0512 $[M-H]^-$ consistent with the molecular formula $C_{15}H_{12}O_7$ (calculated m/z 303.05101 $[M-H]^-$) was detected, indicating the presence of 2-hydroxydihydrokaempferol, which could explain the unexpected detection of kaempferol. However, the assignment could not be confirmed because no authentic 2-hydroxydihydrokaempferol

standard was commercially available. In addition, very low signals possibly belonging to 2-hydroxygarbanzol (no commercial standard available) were detected. None of these signals were present in the negative control *S. albus* pLAGO.

Quantification of the intermediates and final products obtained with *S. albus* pGR led to the identification of *p*-coumaric acid ($694.65 \pm 9.52 \mu\text{g l}^{-1}$), as well as lower concentrations of dihydrokaempferol ($53.95 \pm 0.84 \mu\text{g l}^{-1}$), liquiritigenin ($40.48 \pm 1.81 \mu\text{g l}^{-1}$), naringenin ($38.52 \pm 0.62 \mu\text{g l}^{-1}$), isoliquiritigenin ($19.081 \pm 0.17 \mu\text{g l}^{-1}$), garbanzol ($3.74 \pm 0.55 \mu\text{g l}^{-1}$), kaempferol ($1.74 \pm 0.08 \mu\text{g l}^{-1}$), apigenin ($0.36 \pm 0.01 \mu\text{g l}^{-1}$), 2-hydroxynaringenin ($0.32 \pm 0.05 \mu\text{g l}^{-1}$), resokaempferol ($0.14 \pm 0.016 \mu\text{g l}^{-1}$) and 7,4'-dihydroxyflavone ($0.002 \pm 0.0003 \mu\text{g l}^{-1}$) (Fig. S3).

When the *S. albus* pGR strain was supplemented with 0.1 mM of naringenin, the garbanzol yield was drastically reduced ($0.41 \pm 0.04 \mu\text{g l}^{-1}$). The same was true for liquiritigenin ($12.16 \pm 1.12 \mu\text{g l}^{-1}$), 7,4'-dihydroxyflavone (LOQ, limit of quantification) and resokaempferol (LOQ), whereas titres of apigenin ($2.82 \pm 0.09 \mu\text{g l}^{-1}$) and kaempferol ($2.45 \pm 0.41 \mu\text{g l}^{-1}$) increased; titres of *p*-coumaric acid ($753.40 \pm 10.23 \mu\text{g l}^{-1}$), isoliquiritigenin ($14.35 \pm 0.29 \mu\text{g l}^{-1}$) and dihydrokaempferol ($46.91 \pm 2.26 \mu\text{g l}^{-1}$) remained unaltered (Fig. S3).

Heterologous biosynthesis of fustin

Fustin is a hydroxylated derivative of garbanzol, and its biosynthesis requires the activity of one additional enzyme (F3'H) able to hydroxylate garbanzol at C3'. After having checked that the *S. albus* host was able to produce garbanzol, the gene coding for the F3'H enzyme was cloned into pGR (Fig. 2B). The new plasmid pDF was used for the transformation of *S. albus*, and the crude extract obtained after cultivation of the recombinant strain was subjected to HPLC-HRESIMS analysis.

As expected, all final products and the intermediates of the pathway that have been previously described for *S. albus* pGR were also detected in *S. albus*-harbouring pDF, including the 2-hydroxy intermediates 2-hydroxyliquiritigenin, 2-hydroxynaringenin (Fig. S2C) and putative 2-hydroxydihydrokaempferol. Regarding the differential peaks from *S. albus* pGR, clear signals arose at m/z 287.0565/287.0558 $[M-H]^-$ (two signals with different retention times), m/z 285.0402 $[M-H]^-$, m/z 271.0615 $[M-H]^-$, m/z 303.0505 $[M-H]^-$ and m/z 301.0350 $[M-H]^-$, which had the same retention time as authentic fustin (calculated m/z 287.05610 $[M-H]^-$; $C_{15}H_{12}O_6$), eriodictyol (calculated m/z 287.05610 $[M-H]^-$; $C_{15}H_{12}O_6$), fisetin (calculated m/z 285.04045 $[M-H]^-$; $C_{15}H_{10}O_6$), butin (calculated m/z 271.06118 $[M-H]^-$; $C_{15}H_{12}O_5$),

dihydroquercetin (calculated m/z 303.05101 [M-H]⁻ C₁₅H₁₂O₇) and quercetin (calculated m/z 301.03536 [M-H]⁻; C₁₅H₁₀O₇) respectively (Fig. S2C). All these differential peaks result from the activity of F3'H, which can use naringenin, dihydrokaempferol, kaempferol, liquiritigenin and garbanzol as substrates, and its activity was described in a previous study by our group (Marín *et al.*, 2018).

For *S. albus* pDF, product titres were similar to *S. albus* pGR: *p*-coumaric acid ($672.80 \pm 19.34 \mu\text{g l}^{-1}$), dihydrokaempferol ($47.32 \pm 4.73 \mu\text{g l}^{-1}$), liquiritigenin ($35.12 \pm 0.007 \mu\text{g l}^{-1}$), naringenin ($34.41 \pm 2.17 \mu\text{g l}^{-1}$), isoliquiritigenin ($17.22 \pm 0.31 \mu\text{g l}^{-1}$), garbanzol ($2.69 \pm 0.19 \mu\text{g l}^{-1}$), kaempferol ($1.30 \pm 0.23 \mu\text{g l}^{-1}$), apigenin ($0.25 \pm 0.02 \mu\text{g l}^{-1}$), 2-hydroxynaringenin ($0.19 \pm 0.09 \mu\text{g l}^{-1}$), resokaempferol ($0.12 \pm 0.02 \mu\text{g l}^{-1}$) and 7,4'-dihydroxyflavone ($0.002 \pm 0.0003 \mu\text{g l}^{-1}$). Also, fustin ($0.45 \pm 0.10 \mu\text{g l}^{-1}$), dihydroquercetin ($3.57 \pm 1.27 \mu\text{g l}^{-1}$) and quercetin ($0.07 \pm 0.04 \mu\text{g l}^{-1}$) were detected due to F3'H activity (Fig. S3).

Discussion

Previous studies of our research group have demonstrated *de novo* production of several flavonoids derived from naringenin chalcone in *S. albus* (Fig. 1A; Marín *et al.*, 2017, 2018; García-Gutiérrez *et al.*, 2020). However, the present work describes *de novo* biosynthesis of flavonoids from a 6'-deoxychalcone produced by the activity of CHR. To our knowledge, flavonoid biosynthesis in the genus *Streptomyces* has focussed on naringenin or pinocembrin chalcone derivatives (Park *et al.*, 2009, 2010, 2011), and heterologous production of isoliquiritigenin derivatives such as garbanzol, fustin or resokaempferol has not yet been described in these actinomycetes (Rozmer and Perjési, 2016; Fig. 1B). To achieve an engineered production of garbanzol and fustin without supplementation of intermediates, the different genes that configure the biosynthetic pathway of these flavanones were cloned and expressed in the recombinant strains *S. albus* pGR and *S. albus* pDF, but different pathway intermediates and shunt products were hitherto detected (see Appendix S1; Fig. S3).

Six peaks consistent with a molecular formula of C₁₅H₁₂O₅ were identified (Fig. 3A), with peaks 2 and 6 assigned as garbanzol and naringenin respectively. Hence, we hypothesized that peaks 1, 3, 4 and 5 could be isomers related to the biosynthetic pathway of garbanzol, and peak 1 (Fig. 3A) was putatively identified as 2-hydroxyliquiritigenin, an extremely rare natural product suggested to be an intermediate in the conversion of flavanones to flavones (Jiang *et al.*, 2019; Yonekura-Sakakibara *et al.*, 2019; Fig. 1B) The close relationship between garbanzol and putative 2-hydroxyliquiritigenin

was evidenced when *S. albus* pGR strain was monitored over time because maximum intensities of both peaks switched over time (72 h and 168 h respectively; Fig. S5).

It was not possible to perform the structural elucidation of putative 2-hydroxyliquiritigenin by NMR due to problems related to its instability under the tested conditions. In fact, it is said that 2-hydroxyflavanones exist together with dibenzoylmethanes as tautomeric mixtures (keto- and enol forms) in specific solvents such as DMSO and acetone, generating overlapping signals that cannot be assigned to one or the other tautomer with certainty (Stevens *et al.*, 1999; Ti *et al.*, 2011). Although NMR analysis generated a broad spectrum with more signals than would be expected for an individual molecule structure, peak 1 (in Fig. 3A) could be traced back based on the absence of signals from oxygenated methines in the mixture, as well as on its UV/vis and fragmentation spectrum (see Appendix S1). Unfortunately, 2-hydroxyliquiritigenin was not commercially available, and its fragmentation profile was published in metabolomic databases such as FlavonoidSearch (Akimoto *et al.*, 2017).

The existence of 2-hydroxyliquiritigenin in the crude extracts of *S. albus* pGR and *S. albus* pDF was completely unexpected because the introduced biosynthetic pathway lacks the enzymes needed to introduce a hydroxyl group in a position other than C3. In order to understand these surprising results, it is necessary to introduce the biosynthetic pathway of 2-hydroxyliquiritigenin, which is produced from liquiritigenin by the activity of the cytochrome P450-dependent enzyme flavanone 2-hydroxylase (F2H, EC 1.14.14.162), which is unstable and generates licodione by spontaneous hemiacetal opening (Aoki *et al.*, 2000). Alternatively, 2-hydroxyliquiritigenin gives rise to 7,4'-dihydroxyflavone, either by acid treatment or by the action of a dehydratase (Fig. 1B; Akashi *et al.*, 1998; Du *et al.*, 2010). The hypothesis on the presence of this alternative route branching off from liquiritigenin was verified because 7,4'-dihydroxyflavone and licodione (tentative identification, no commercial standard available) were detected in the crude extracts of *S. albus* pGR and *S. albus* pDF (Fig. S2B and C). Additionally, new flavonols (resokaempferol and kaempferol) were identified as well as 2-hydroxy intermediates other than 2-hydroxyliquiritigenin (2-hydroxynaringenin and putative 2-hydroxydihydrokaempferol; Fig. S2A). The synthesis of flavones or 2-hydroxyflavanones was surprising because no F2H-, FNS- or flavonol synthase (FLS, EC 1.14.20.6)-encoding genes were expressed in either of these strains.

In order to discard the potential presence of a gene coding for a native F2H enzyme in the chromosome of

S. albus wild-type strain, a feeding experiment with 0.1 mM naringenin was carried out, but no 2-hydroxynaringenin was observed, ruling out a possible endogenous F2H activity in this bacterium. Moreover, when *S. albus* pGR was supplemented with naringenin, a 10-fold decrease of final garbanzol titres was obtained and the 2-hydroxyliquiritigenin signal almost disappeared, whereas the amount of dihydrokaempferol and its derivatives increased. As it will be further discussed, we think that F3H has a F2H side activity because F3H is acting on naringenin substrate under feeding conditions, rather than on liquiritigenin to generate 2-hydroxyliquiritigenin (Figs 1 and S3).

Interestingly, F2H activity can also be obtained by other enzymes such as flavone synthases (FNSs): FNSI (soluble Fe²⁺/2-oxoglutarate-dependent dioxygenase, EC 1.14.20.5) and FNSII (NADPH-dependent cytochrome P450 membrane-bound monooxygenase, EC 1.14.19.76; Martens and Mithöfer, 2005). They are responsible for catalysing the conversion of flavanones to flavones by introducing a double bond between C2 and C3 in the heterocycle (Britsch, 1990; Zhang *et al.*, 2007; Jiang *et al.*, 2019), but some FNSII can also exhibit F2H activity, being required the activity of an additional unknown dehydratase to generate the flavone *in planta* (Akashi *et al.*, 1999; Du *et al.*, 2010; Wu *et al.*, 2016). This said, the attention then focused on F3H as it is a 2-oxoglutarate-dependent oxygenase closely related to FNSI, being the only enzyme in the cloned pathway being able to catalyse the hydroxylation of the heterocycle. We believe that there is a relationship between F3H and FNSI, which could explain an additional F2H activity. Evolutionary relationship of enzymes and *in vivo* and *in vitro* studies may support this hypothesis. Firstly, F3H and FNSI share a 90% protein identity, and their tertiary structure is highly similar (Cheng *et al.*, 2014; Park *et al.*, 2019). Moreover, Gebhardt *et al.* (2007) demonstrated by site-directed mutagenesis a complete change of activity from F3H to FNSI, leading to production of apigenin from naringenin, instead of dihydrokaempferol production (Gebhardt *et al.*, 2005, 2007). Secondly, it was recently described that a bryophyte FNSI not only generated apigenin from naringenin directly as it was traditionally thought but also showed F2H activity to produce 2-hydroxynaringenin. Moreover, the bryophyte enzyme also generated kaempferol from dihydrokaempferol, demonstrating that FNSIs can also act as FLS enzymes by recognizing not only flavanones but also flavanonols (Han *et al.*, 2014). In relation to the catalytic activity of the F3H enzyme used in the present work, it has been shown that it lacks FNS or FLS activity and cannot generate apigenin or kaempferol from naringenin or dihydrokaempferol, respectively

(Wellmann *et al.*, 2004; Shen *et al.*, 2010); however, as far as we know, there are no references to its suspected F2H activity.

Therefore, the close evolutionary relationship between F3H and FNSI, along with the F2H activity described for an FNSI, leads us to hypothesize that our F3H (encoded in pGR and pDF recombinant vectors) can have an F2H side activity allowing the formation of 2-hydroxyliquiritigenin and 2-hydroxynaringenin (spectrum signals coming from putative 2-hydroxydihydrokaempferol were also detected, but no commercial standard was available). Finally, an endogenous *S. albus* dehydratase would be responsible for generating the corresponding flavones (apigenin and 7,4'-dihydroxyflavone) or flavonols (kaempferol or resokaempferol) from its 2-hydroxy precursors because FNSI (as well as FNSII) does not accept 2-hydroxy derivatives as substrates *in vitro* (Zhang *et al.*, 2007; Han *et al.*, 2014; Fig. 1). Our hypothesis involving a native *S. albus* dehydratase is similar to what has been observed in cultures of *Saccharomyces* sp. supplemented with naringenin because the heterologous expression of a gene encoding the *Medicago truncatula* FNSII led to flavone production *in vivo*, but it only yielded 2-hydroxynaringenin *in vitro* (Akashi *et al.*, 1999; Zhang *et al.*, 2007). The side activity of some flavonoid enzymes is not entirely new; in fact, it has been described that some FLSs present F3H activity, despite the low homology that exists between both enzymes (Prescott *et al.*, 2002; Duan *et al.*, 2017; Park *et al.*, 2019; Sun *et al.*, 2019).

The strain *S. albus* J1074 has been widely used as a workhorse for heterologous production of a wide range of natural products over the last two decades (Lombó *et al.*, 2006; Myronovskiy *et al.*, 2016; Liu *et al.*, 2018; Fazal *et al.*, 2020) and could be regarded as a promising platform for heterologous flavonoid expression, but multiple genome improvements are needed. Firstly, improvements focused on increasing the intracellular availability of the main bottleneck in flavonoid biosynthesis (malonyl-CoA) would be necessary (Takamura and Nomura, 1988; Kurth *et al.*, 2009; Santos *et al.*, 2011), as well as limiting its use by other native biosynthetic clusters (Myronovskiy *et al.*, 2018). On the other hand, the fact that a negative control strain supplemented with naringenin generated apigenin and eriodictyol (see Appendix S1) makes necessary to identify and to silence the promiscuous activities (Verdel-Aranda *et al.*, 2015; Esnault *et al.*, 2017). Deletion of endogenous catabolic pathways responsible for the degradation of L-Tyr would also increase the cytoplasmic pool of building blocks for flavonoid biosynthesis in this strain (Jiang *et al.*, 2005; Kim *et al.*, 2018). All these efforts will consolidate the use of *S. albus* as a highly attractive host for production of flavonoids.

In conclusion, our experiments demonstrated the functional introduction of 4 different biosynthetic pathways branching off from naringenin or isoliquiritigenin into the actinomycete *S. albus*. When using naringenin as a substrate, apigenin (2-hydroxynaringenin as an intermediate), kaempferol (dihydrokaempferol and 2-hydroxydihydrokaempferol as intermediates) and quercetin (kaempferol as an intermediate) were obtained. In a related approach, resokaempferol (garbanzol and putative 2-hydroxygarbanzol as intermediates), putative licodione (2-hydroxyliquiritigenin as an intermediate), 7,4'-dihydroxyflavone (2-hydroxyliquiritigenin as an intermediate) and fustin (garbanzol as an intermediate) were biosynthesized from liquiritigenin (Fig. 1). The functional introduction of a pathway leading to putative licodione, 2-hydroxyliquiritigenin or 7,4'-dihydroxyflavone has never been reported in a microbial host before. The competitive effects between the four branches of this complex biosynthetic pathway, in which naringenin and liquiritigenin both serve as substrates of F3H, can explain the high structural diversity of flavonoids achieved in this bacterial factory as well as the low titres of the expected end-products.

Experimental procedures

Bacterial strains, plasmids and culture conditions

All strains and plasmids used in this study are listed in Table 1. *E. coli* TOP10 (Invitrogen), pSL1180 (Brosius, 1989) and pUC57 (Fermentas) were used for routine subcloning. The strain *Streptomyces albus* J1074, a mutant of the *S. albus* G strain that lacks an active *Sall* restriction modification system, was used for the production of flavonoids (Chater and Wilde, 1980). The high copy number *E. coli*-*Streptomyces* shuttle vector pIAGO, which harbours the strong constitutive promoter of *ermE** (*PermE**), was chosen as the expression plasmid (Aguirrezabalaga *et al.*, 2000) as this assures high expression levels in the host. This vector harbours the pJ101 origin of replication from *S. lividans* ISP5434, which assures around 300 copies per chromosome, or 30% of the total strain DNA (Kieser *et al.*, 2000). The promoter P_{ermE} is derived from the promoter region of the erythromycin resistance gene (*ermE*) of the erythromycin producer *Streptomyces erythraeus* (Bibb *et al.*, 1985), which actually contains two different promoters, P_{ermE1} and P_{ermE2} , and the *PermE** promoter is a stronger variant containing the P_{ermE2} and a TGG deletion in the -35 region of the P_{ermE1} part.

E. coli strains were grown in tryptic soy broth (TSB, VWR) or on TSB agar plates, supplemented with the corresponding antibiotic (ampicillin 100 $\mu\text{g ml}^{-1}$, Sigma Aldrich, Madrid, Spain) for maintenance of the plasmid. *S. albus* J1074 was grown at 30°C in yeast extract–malt

Table 1. Plasmids and strains used in this study.

	Description	Source
Plasmid		
pIAGO	pWHM3 (replicative shuttle vector) carrying <i>ermE</i> * promoter	Aguirrezabalaga <i>et al.</i> (2000)
pSL1180	<i>E. coli</i> vector	Brosius (1989)
pUC57	<i>E. coli</i> vector	Fermentas
pLMF1	pUC57 carrying <i>TAL</i>	This study
pLMF2	pUC57 carrying <i>4CL</i>	This study
pLMF3	pUC57 carrying <i>CHS</i>	This study
pLMF4	pUC57 carrying <i>CHR</i>	This study
pLMF5	pUC57 carrying <i>CHI</i>	This study
pLMF7	pSL1180 carrying <i>TAL</i>	This study
pLMF8	pSL1180 carrying <i>TAL</i> and <i>4CL</i>	This study
pLMF11	pUC57 carrying <i>CHS</i> and <i>CHR</i>	This study
pLMF-F3H	pUC57 carrying <i>F3H</i>	This study
pLMF-F3'H	pUC57 carrying <i>F3'H</i>	This study
pLMF14	pSL1180 carrying <i>TAL</i> , <i>4CL</i> , <i>CHS</i> and <i>CHR</i>	This study
pLMF15	pUC57 carrying <i>CHI</i> and <i>F3H</i>	This study
pLMF18	pSL1180 carrying <i>TAL</i> , <i>4CL</i> , <i>CHS</i> , <i>CHR</i> , <i>CHI</i> and <i>F3H</i>	This study
pLMF19	pSL1180 carrying <i>TAL</i> , <i>4CL</i> , <i>CHS</i> , <i>CHR</i> , <i>CHI</i> , <i>F3H</i> and <i>F3'H</i>	This study
pGR	pIAGO carrying <i>TAL</i> , <i>4CL</i> , <i>CHS</i> , <i>CHR</i> , <i>CHI</i> and <i>F3H</i>	This study
pDF	pIAGO carrying <i>TAL</i> , <i>4CL</i> , <i>CHS</i> , <i>CHR</i> , <i>CHI</i> , <i>F3H</i> and <i>F3'H</i>	This study
Strains		
<i>E. coli</i> TOP10	Strain used for routine subcloning	Invitrogen
<i>Streptomyces albus</i> J1074	Strain used to create the flavonol-producing clones	Chater and Wilde (1980)
<i>S. albus</i> -pIAGO	<i>S. albus</i> harbouring pIAGO used as negative control	This study
<i>S. albus</i> -pGR	<i>S. albus</i> carrying pGR	This study
<i>S. albus</i> -pDF	<i>S. albus</i> carrying pDF	This study

extract (YEME) 17% (w/v) sucrose for the preparation of protoplasts. It was sporulated in Bennett medium (Kieser *et al.*, 2000) and supplemented with the corresponding antibiotics, when necessary (thiostrepton 50 $\mu\text{g ml}^{-1}$, Cayman Chemical, Ann Arbor, MI, USA).

For flavonoid production, *S. albus* spores were quantified, and a pre-inoculum of 10^7 spores ml^{-1} was transferred into Bennett medium which was first incubated for 72 h until sporulation and subsequently transferred to 30 ml of liquid R5A medium (Fernández *et al.*, 1998). The cultures were incubated for 84 h at 30°C and 250 revolutions per minute (rpm). In the feeding experiments, 0.1 mM of naringenin was added after 24 h of incubation. When higher culture volumes for 2-hydroxyliquiritigenin purification were needed, the volume was scaled up to 6 l. In these cases, a pre-inoculum was made in liquid R5A medium with 10^7 spores ml^{-1} , incubated for 45 h at 30°C and

250 r.p.m., and a 10% (v/v) inoculum size was finally used for 6 l final culture volume and incubated for 112 h at 30°C and 250 r.p.m.

For *S. albus* pGR growth and production curves, triplicate cultures of *S. albus* pGR were grown in shake flasks with 30 ml of R5A over a duration of 168 h. Samples were taken every 24 h per duplicate to determine biomass as dry cell weight as well as production titres of garbanzol, liquiritigenin and isoliquiritigenin.

Reagents and biochemicals

All solvents used for solid-phase extraction, HPLC analysis/purification and MS-based experiments were LC-MS grade from either Sigma-Aldrich or VWR Chemicals. Authentic standards for LC-HRESIMS quantification and molecule identification through LC-HRESIMS and LC-UV/vis were purchased from different suppliers: *p*-coumaric acid (Sigma Aldrich, USA), naringenin (Sigma Aldrich, USA), dihydrokaempferol (Sigma Aldrich, USA), kaempferol (Cayman Chemical, USA), apigenin (Extrasynthese, Genay, France), 2-hydroxynaringenin (Ambinter, Orléans, France), isoliquiritigenin (Sigma Aldrich, USA), liquiritigenin (Tocris Bioscience, Bristol, UK), (2*R*,3*R*)-garbanzol (BioBioPha, Kunming, Yunnan, China), (2*S*,3*S*)-garbanzol (AnalytiCon Discovery, Potsdam, Germany), resokaempferol (Extrasynthese), fustin (Biosynth Carbosynth, Compton, UK), butin (ChemFaces, Wuhan, China), 7,4'-dihydroxyflavone (Extrasynthese, France), quercetin (Cayman Chemical) and dihydroquercetin (Sigma Aldrich).

Genes and enzymes

Recombinant DNA techniques were performed following standard protocols (Sambrook and Russell, 2001). Restriction enzymes were purchased from Takara Biochemicals, T4 DNA ligase from Thermo Scientific and DreamTaq DNA Polymerase from Thermo Scientific. Synthetic genes for the following ORFs were synthesized by GenScript after codon optimization: *TAL* from *Rhodobacter capsulatus* (Genbank accession no. WP_013066811), *4CL* from *S. coelicolor* (Genbank accession no. NP_628552), *CHS* from *Glycine max* (Genbank accession no. L07647.1), *CHR* from *G. max* (Genbank accession no. X55730.1), *CHI* from *G. max* (Genbank accession no. AY595413.1), *F3H* from *Petroselinum crispum* (Genbank accession no. AY23248) and *F3'H* from *A. thaliana* (Genbank accession no. Q9SD85). Genbank accession numbers LT629805.1, LT629806.1, LT629807.1, MW404307, LT629808.1, LT629809.1 and MG748610 belong to the synthetic genes encoding *TAL*, *4CL*, *CHS*, *CHR*, *CHI*, *F3'H* and *F3H* respectively. Compatible restriction sites were

added at each the gene cassette end and ribosome-binding sites at the 5'-ends. The RBS sequence (in bold) for all genes was 5'-TCCCGT**AGGAGG**ACGAC-3'.

All constructed plasmids described later were verified by restriction enzyme digestions and also by sequencing of the cloned regions. Recombinant *Streptomyces* clones were confirmed by PCR. Primers used to amplify the first two common genes included 5'-GTGATCGAGCTGGA CATGAA-3' as the forward primer and 5'-GGCGTCC ACGAGGTGC-3' as the reverse primer.

Construction of pGR

The plasmid pGR contains the *ermE** promoter (PerME*) and the six genes encoding enzymes responsible for garbanzol biosynthesis. All synthetic gene cassettes were independently cloned in pUC57, and plasmids were named pLMF1 (pUC57 containing *TAL* gene), pLMF2 (*4CL*), pLMF3 (*CHS*), pLMF4 (*CHR*), pLMF5 (*CHI*) and pLMF-F3H (*F3H*) (Table 1). Additionally, the *TAL* gene was subcloned into vector pSL1180 using *HindIII-BamHI* (pLMF7) in the first step of the cloning strategy. The *4CL* gene (from pLMF2) was cloned into pLMF7 as *PstI-BamHI* gene cassette, generating pLMF8. The next step included subcloning of the *CHR* gene cassette from pLMF4 into pLMF3 using *EcoRI*, yielding pLMF11. The correct orientation of each DNA fragment was confirmed after each step by restriction enzyme digestions and sequencing. The two gene cassettes from pLMF11 (*CHS* and *CHR*) were subcloned together into pLMF8 using *SacI-BamHI* in order to assemble the first four genes in a plasmid (pLMF14). Finally, the *F3H* gene was subcloned into pLMF5 (cut with *EcoRV-BamHI*) as an *EcoRI* (blunt-ended)-*BamHI* gene cassette, and the ligation product (harbouring the genes *CHI* and *F3H*) was subcloned into pLMF14 using *XbaI-BamHI*, resulting in pLMF18, which contains the six genes required for garbanzol biosynthesis. As the expression host was *Streptomyces*, a further subcloning step was required, in which the *BglII-BamHI* DNA fragment carrying the six genes was finally subcloned into the pIAGO plasmid (Fig. 2A), a derivative of the bifunctional replicative vector pWHM3, which contains the *ermE** promoter, giving rise to the final plasmid pGR.

Construction of pDF

The plasmid pDF contains the *ermE** promoter (PerME*) and the seven genes required for the biosynthesis of fustin. To obtain this plasmid, it was required to add one more gene to the previous plasmid pLMF18 constructed to produce garbanzol. This last gene, *F3'H*, was cloned into pLMF18 as *DraI-BamHI* gene cassette, giving rise to pLMF19. The DNA fragment containing seven genes

was subcloned into the vector pIAGO to be further expressed in *Streptomyces* (Fig. 2B). The gene cassette was cloned as a *Bgl*III-*Bam*HI DNA fragment to obtain plasmid pDF (Table 1).

Flavonoid extraction and LC-HRESIMS analysis

S. albus J1074 clones harbouring pGR, pDF or pIAGO (negative control) were incubated (three replicates for each strain) as described earlier. The recovery of flavonoids from the recombinant strains developed in this study was achieved by an organic extraction with acetone (cellular pellet) and ethyl acetate (culture supernatant). Briefly, 30 ml of culture medium was centrifuged at 10 000 r.p.m. for 5 min, and the biomass and the supernatant were extracted separately. Firstly, an equal volume of acetone was added to the pellet to facilitate the breaking of the mycelium and then a second extraction was performed with an equal volume of ethyl acetate. For the supernatant, two extractions were performed with the same volume of ethyl acetate. Finally, the organic phases were dried sequentially under vacuum in a rotavapor (RV 10 Digital, IKA) equipped with a vertical condenser maintained at -10°C (RC-10 Digital Chiller, VWR) and brought together in a single 10 ml glass vial.

For the identification of flavonoids using HPLC-HRESIMS, the dry extract obtained was reconstituted in 200 μl DMSO/MeOH 1:1 (v/v), and the samples were processed sequentially through 0.8 and 0.2 μm filters (Acrodisc[®], Pall). Separation was performed in a UPLC system (Dionex Ultimate 3000, ThermoScientific, Madrid, Spain) equipped with an analytical RP-18 HPLC column (50 \times 2.1 mm, Zorbax[®] Eclipse Plus, 1.8 μm , Agilent Technologies, Madrid, Spain) heated to 30°C , and a combination of distilled water (mobile phase A) and MeCN (mobile phase B), both acidified with 0.1% (v/v) of formic acid, was used. The analytes were eluted at a flow rate of 0.25 ml min^{-1} in a 10–100% (v/v) gradient of MeCN under the following conditions: 0–1 min (10% B), 1–4 min (10–35% B), 4–5 min (35% B), 5–8 min (35–100% B), 8–10 min (100% B), 1011 min (100–10% B) and 11–15 min (10% B). The column effluent was directed to electrospray ionization mass spectrometry analysis (HPLC-ESI-MS) using an ESI-UHR-Qq-TOF Impact II spectrometer (Bruker Española SA, Madrid, Spain) which acquired data in the negative ion mode, with a m/z range from 40 to 2000 Da. Data were analysed using Compass DataAnalysis 4.3 (Bruker). The obtained BPCs were extracted for the deprotonated ions of a set of flavonoids with a mass error range of 0.005 mmu (milli mass units), and the obtained EICs (extracted ion chromatograms) were compared with

authentic commercial standards. When needed, flavonoids were quantified by comparing the peak area with that of a known amount of an authentic compound through a calibration curve. The production titres are given in $\mu\text{g/L}$, and the mean value was calculated from three biological replicates.

Purification and elucidation of 2-hydroxyliquiritigenin

In order to obtain sufficient amounts of 2-hydroxyliquiritigenin for structural elucidation, the production volume of *S. albus* pGR was scaled up, and the culture was subsequently extracted. The extraction method was followed as described earlier, with the only difference that the supernatant was extracted four times and a 2 l separating funnel was used to separate the organic from the aqueous phase. Finally, 4.03 g of dry residue were obtained, which was then subjected to HRESIMS-guided fractionation: a first phase of pre-fractionation by solid-phase extraction (SPE) was needed, followed by two HPLC-UV/vis purification rounds under semi-preparative conditions (see Appendix S1).

Statistical methods

A two-way ANOVA was used to compare cultivation data of *S. albus* pGR and negative control *S. albus* pIAGO. Considering that each row represents a different incubation time, matched values were stacked into a sub-column, and a Šidák correction was used, which has a higher statistical power than Bonferroni correction. The alpha threshold and confidence level selected for data was of 0.05 (95% confidence level). The graphic representation of all the cultivation data was carried out using GRAPHPAD PRISM software (version 7, GraphPad Software, San Diego, CA, USA).

Acknowledgements

The University of Oviedo thanks *Programa de Ayudas a Grupos de Investigación del Principado de Asturias* (IDI/2018/000120), *Programa Severo Ochoa de Ayudas Pre-doctorales para la investigación y docencia* from *Principado de Asturias* (grant BP16023 to I.G.R.), *Proyectos I + D+I, del Programa Estatal de Investigación, Desarrollo e Innovación Orientada a los Retos de la Sociedad*, from *Ministerio de Ciencia, Innovación y Universidades* of Spain (AGL2017-88095-R) and the European Union's Horizon 2020 Research and Innovation Programme under Grant Agreement no. 814650 for the project SynBio4Flav. HRESIMS experiments were conducted at the Mass spectrometry unit of *Servicios Científico-Técnicos* at the University of Oviedo.

Conflict of interest

The authors declare no conflict of interest.

References

- Aguirrezabalaga, I., Olano, C., Allende, N., Rodriguez, L., Braña, A.F., Méndez, C., and Salas, J.A. (2000) Identification and expression of genes involved in biosynthesis of L-oleandrose and its intermediate L-olivose in the oleandomycin producer *Streptomyces antibioticus*. *Antimicrob Agents Chemother* **44**: 1266–1275.
- Akashi, T., Aoki, T., and Ayabe, S. (1998) Identification of a cytochrome P450 cDNA encoding (2 S)-flavanone 2-hydroxylase of licorice (*Glycyrrhiza echinata* L.; Fabaceae) which represents licodione synthase and flavone synthase II¹. *FEBS Lett* **431**: 287–290.
- Akashi, T., Aoki, T., and Ayabe, S.I. (1999) Cloning and functional expression of a cytochrome p450 cDNA encoding 2-hydroxyisoflavanone synthase involved in biosynthesis of the isoflavonoid skeleton in licorice. *Plant Physiol* **121**: 821–828.
- Akimoto, N., Ara, T., Nakajima, D., Suda, K., Ikeda, C., Takahashi, S., et al. (2017) FlavonoidSearch: a system for comprehensive flavonoid annotation by mass spectrometry. *Sci Rep* **7**: 1–9.
- Aoki, T., Akashi, T., and Ayabe, S. (2000) Flavonoids of leguminous plants: structure, biological activity, and biosynthesis. *J Plant Res* **113**: 475–488.
- Bibb, M.J., Janssen, G.R., and Ward, J.M. (1985) Cloning and analysis of the promoter region of the erythromycin resistance gene (ermE) of *Streptomyces erythraeus*. *Gene* **38**: 215–226.
- Britsch, L. (1990) Purification and characterization of flavone synthase I, a 2-oxoglutarate-dependent desaturase. *Arch Biochem Biophys* **282**: 152–160.
- Brosius, J. (1989) Superpolylinkers in cloning and expression vectors. *DNA* **8**: 759–777.
- Buchanan, M.S., Carroll, A.R., Fechner, G.A., Boyle, A., Simpson, M., Addepalli, R., et al. (2008) Small-molecule inhibitors of the cancer target, isoprenylcysteine carboxyl methyltransferase, from *Hovea parvicalyx*. *Phytochemistry* **69**: 1886–1889.
- Chater, K.F., and Wilde, L.C. (1980) *Streptomyces albus* G mutants defective in the SalGI restriction-modification system. *J Gen Microbiol* **116**: 323–334.
- Chen, H., Wang, C., Zhou, H., Tao, R., Ye, J., and Li, W. (2017) Antioxidant capacity and identification of the constituents of ethyl acetate fraction from *Rhus verniciflua* Stokes by HPLC-MS. *Nat Prod Res* **31**: 1573–1577.
- Cheng, A.X., Han, X.J., Wu, Y.F., and Lou, H.X. (2014) The function and catalysis of 2-oxoglutarate-dependent oxygenases involved in plant flavonoid biosynthesis. *Int J Mol Sci* **15**: 1080–1095.
- Chouhan, S., Sharma, K., Zha, J., Guleria, S., and Koffas, M.A.G. (2017) Recent advances in the recombinant biosynthesis of polyphenols. *Front Microbiol* **8**: 2259.
- Crozier, A., Jaganath, I.B., and Clifford, M.N. (2009) Dietary phenolics: chemistry, bioavailability and effects on health. *Nat Prod Rep* **26**: 1001–1043.
- Du, Y., Chu, H., Wang, M., Chu, I.K., and Lo, C. (2010) Identification of flavone phytoalexins and a pathogen-inducible flavone synthase II gene (SbFNSII) in sorghum. *J Exp Bot* **61**: 983–994.
- Duan, L., Ding, W., Liu, X., Cheng, X., Cai, J., Hua, E., and Jiang, H. (2017) Biosynthesis and engineering of kaempferol in *Saccharomyces cerevisiae*. *Microb Cell Fact* **16**: 165.
- Esnault, C., Leiber, D., Toffano-Nioche, C., Tanfin, Z., and Virolle, M.J. (2017) Another example of enzymatic promiscuity: the polyphosphate kinase of *Streptomyces lividans* is endowed with phospholipase D activity. *Appl Microbiol Biotechnol* **101**: 139–145.
- Falcone Ferreyra, M.L., Rius, S.P., and Casati, P. (2012) Flavonoids: biosynthesis, biological functions, and biotechnological applications. *Front Plant Sci* **3**: 1–15.
- Fazal, A., Thankachan, D., Harris, E., and Seipke, R.F. (2020) A chromatogram-simplified *Streptomyces albus* host for heterologous production of natural products. *Antonie Van Leeuwenhoek* **113**: 511–520.
- Fernández, E., Weissbach, U., Reillo, S., Braña, F., Méndez, C., Rohr, J., and Salas, J. (1998) Identification of two genes from *Streptomyces argillaceus* encoding glycosyltransferases involved in transfer of a disaccharide during biosynthesis of the antitumor drug mithramycin. *Journal Bacteriol* **180**: 4929–4937.
- Fernández, J., Redondo-Blanco, S., Gutiérrez-del-Río, I., Miguélez, E.M., Villar, C.J., and Lombó, F. (2016) Colon microbiota fermentation of dietary prebiotics towards short-chain fatty acids and their roles as anti-inflammatory and antitumour agents: a review. *J Funct Foods* **25**: 511–522.
- Fotso, G.W., Kamga, J., Ngameni, B., Uesugi, S., Ohno, M., Kimura, K.-I., et al. (2017) Secondary metabolites with antiproliferative effects from *Albizia glaberrima* var *glabrescens* Oliv. (Mimosoideae). *Nat Prod Res* **31**: 1981–1987.
- García-Gutiérrez, C., Aparicio, T., Torres, L., Martínez-García, E., Lorenzo, V., Villar, C.J., and Lombó, F. (2020) Multifunctional SEVA shuttle vectors for actinomycetes and Gram-negative bacteria. *Microbiol Open* **9**: 1135–1149.
- Gebhardt, Y., Witte, S., Forkmann, G., Lukačič, R., Matern, U., and Martens, S. (2005) Molecular evolution of flavonoid dioxygenases in the family Apiaceae. *Phytochemistry* **66**: 1273–1284.
- Gebhardt, Y.H., Witte, S., Steuber, H., Matern, U., and Martens, S. (2007) Evolution of flavone synthase I from Parsley Flavanone 3 β-hydroxylase by site-directed mutagenesis. *Plant Physiol* **144**: 1442–1454.
- Genilloud, O. (2017) Actinomycetes: still a source of novel antibiotics. *Nat Prod Rep* **34**: 1203–1232.
- George, V.C., Dellaire, G., and Rupasinghe, H.P.V. (2017) Plant flavonoids in cancer chemoprevention: role in genome stability. *J Nutr Biochem* **45**: 1–14.
- Gutiérrez-del-Río, I., Fernández, J., and Lombó, F. (2018) Plant nutraceuticals as antimicrobial agents in food preservation: terpenoids, polyphenols and thiols. *Int J Antimicrob Agents* **52**: 309–315.
- Han, X.-J., Wu, Y.-F., Gao, S., Yu, H.-N., Xu, R.-X., Lou, H.-X., and Cheng, A.-X. (2014) Functional

- characterization of a *Plagiochasma appendiculatum* flavone synthase I showing flavanone 2-hydroxylase activity. *FEBS Lett* **588**: 2307–2314.
- Hashida, K., Tabata, M., Kuroda, K., Otsuka, Y., Kubo, S., Makino, R., *et al.* (2014) Phenolic extractives in the trunk of *Toxicodendron vernicifluum*: chemical characteristics, contents and radial distribution. *J Wood Sci* **60**: 160–168.
- Jang, J.Y., Shin, H., Lim, J.-W., Ahn, J.H., Jo, Y.H., Lee, K.Y., *et al.* (2018) Comparison of antibacterial activity and phenolic constituents of bark, lignum, leaves and fruit of *Rhus verniciflua*. *PLoS One* **13**: e0200257.
- Jiang, H., Wood, K.V., and Morgan, J.A. (2005) Metabolic engineering of the phenylpropanoid pathway in *Saccharomyces cerevisiae*. *Appl Environ Microbiol* **71**: 2962–2969.
- Jiang, Y., Ji, X., Duan, L., Ye, P., Yang, J., Zhan, R., *et al.* (2019) Gene mining and identification of a flavone synthase II involved in flavones biosynthesis by transcriptomic analysis and targeted flavonoid profiling in *Chrysanthemum indicum* L. *Ind Crops Prod* **134**: 244–256.
- Jo, S., Kim, S., Shin, D.H., and Kim, M.-S. (2020) Inhibition of SARS-CoV 3CL protease by flavonoids. *J Enzyme Inhib Med Chem* **35**: 145–151.
- Kang, S.Y., Kang, J.-Y., and Oh, M.-J. (2012) Antiviral activities of flavonoids isolated from the bark of *Rhus verniciflua* stokes against fish pathogenic viruses In Vitro. *J Microbiol* **50**: 293–300.
- Kieser, T., Chater, K., Bibb, M., Buttner, M., and Hopwood, D.J. (2000) *Practical Streptomyces Genetics*. England : The John Innes Foundation. ISBN: 978-0-7084-0623-6.
- Kim, B., Binkley, R., Kim, H.U., and Lee, S.Y. (2018) Metabolic engineering of *Escherichia coli* for the enhanced production of L-tyrosine. *Biotechnol Bioeng* **115**: 2554–2564.
- Kumar, S., and Pandey, A.K. (2013) Chemistry and biological activities of flavonoids: an overview. *ScientificWorldJournal* **2013**: 162750.
- Kurth, D.G., Gago, G.M., de la Iglesia, A., Bazet Lyonnet, B., Lin, T.-W., Morbidoni, H.R., *et al.* (2009) ACCase 6 is the essential acetyl-CoA carboxylase involved in fatty acid and mycolic acid biosynthesis in mycobacteria. *Microbiology* **155**: 2664–2675.
- Kyndt, J.A., Meyer, T.E., Cusanovich, M.A., and Van Beeumen, J.J. (2002) Characterization of a bacterial tyrosine ammonia lyase, a biosynthetic enzyme for the photoactive yellow protein. *FEBS Lett* **512**: 240–244.
- Lee, K.M., Lee, K.W., Byun, S., Jung, S.K., Seo, S.K., Heo, Y.-S., *et al.* (2010) 5-Deoxykaempferol plays a potential therapeutic role by targeting multiple signaling pathways in skin cancer. *Cancer Prev Res* **3**: 454–465.
- Li, A., Li, S., Zhang, Y., Xu, X., Chen, Y., and Li, H. (2014) Resources and biological activities of natural polyphenols. *Nutrients* **6**: 6020–6047.
- Li, K.K., Shen, S.S., Deng, X., Shiu, H.T., Siu, W.S., Leung, P.C., *et al.* (2018) Dihydrofisetin exerts its anti-inflammatory effects associated with suppressing ERK/p38 MAPK and Heme Oxygenase-1 activation in lipopolysaccharide-stimulated RAW 264.7 macrophages and carrageenan-induced mice paw edema. *Int Immunopharmacol* **54**: 366–374.
- Liu, C., Weir, D., Busse, P., Yang, N., Zhou, Z., Emala, C., and Li, X.-M. (2015) The Flavonoid 7,4'-dihydroxyflavone inhibits MUC5AC gene expression, production, and secretion via regulation of NF- κ B, STAT6, and HDAC2. *Phyther Res* **29**: 925–932.
- Liu, X., Liu, D., Xu, M., Tao, M., Bai, L., Deng, Z., *et al.* (2018) Reconstitution of Kinamycin Biosynthesis within the Heterologous Host *Streptomyces albus* J1074. *J Nat Prod* **81**: 72–77.
- Lombó, F., Velasco, A., Castro, A., de la Calle, F., Braña, A.F., Sánchez-Puelles, J.M., *et al.* (2006) Deciphering the biosynthesis pathway of the antitumor thiocoraline from a marine actinomycete and its expression in two *Streptomyces* species. *ChemBioChem* **7**: 366–376.
- Marín, L., Gutiérrez-del-Río, I., Yagüe, P., Manteca, Á., Villar, C.J., and Lombó, F. (2017) De novo biosynthesis of apigenin, luteolin, and eriodictyol in the actinomycete *Streptomyces albus* and production improvement by feeding and spore conditioning. *Front Microbiol* **8**: 1–12.
- Marín, L., Gutiérrez-del-Río, I., Entrialgo-Cadierno, R., Claudio, V.J., and Lombó, F. (2018) De novo biosynthesis of myricetin, kaempferol and quercetin in *Streptomyces albus* and *Streptomyces coelicolor*. *PLoS One* **13**: e0207278.
- Martens, S., and Mithöfer, A. (2005) Flavones and flavone synthases. *Phytochemistry* **66**: 2399–2407.
- Matkowski, A. (2008) Plant in vitro culture for the production of antioxidants — a review. *Biotechnol Adv* **26**: 548–560.
- Myronovskiy, M., Brötz, E., Rosenkränzer, B., Manderscheid, N., Tokovenko, B., Rebets, Y., and Luzhetskyy, A. (2016) Generation of new compounds through unbalanced transcription of landomycin A cluster. *Appl Microbiol Biotechnol* **100**: 9175–9186.
- Myronovskiy, M., Rosenkränzer, B., Nadmid, S., Pujic, P., Normand, P., and Luzhetskyy, A. (2018) Generation of a cluster-free *Streptomyces albus* chassis strains for improved heterologous expression of secondary metabolite clusters. *Metab Eng* **49**: 316–324.
- Park, B.C., Lee, Y.S., Park, H.-J., Kwak, M.-K., Yoo, B.K., Kim, J.Y., and Kim, J.-A. (2007) Protective effects of fustin, a flavonoid from *Rhus verniciflua* Stokes, on 6-hydroxydopamine-induced neuronal cell death. *Exp Mol Med* **39**: 316–326.
- Park, K.-Y., Jung, G.-O., Lee, K.-T., Choi, J., Choi, M.-Y., Kim, G.-T., *et al.* (2004) Antimutagenic activity of flavonoids from the heartwood of *Rhus verniciflua*. *J Ethnopharmacol* **90**: 73–79.
- Park, S.R., Ahn, M.S., Han, A.R., Park, J.W., and Yoon, Y.J. (2011) Enhanced flavonoid production in *Streptomyces venezuelae* via metabolic engineering. *J Microbiol Biotechnol* **21**: 1143–1146.
- Park, S., Kim, D.-H., Park, B.-R., Lee, J.-Y., and Lim, S.-H. (2019) Molecular and functional characterization of *Oryza sativa* Flavonol Synthase (OsFSL), a bifunctional dioxygenase. *J Agric Food Chem* **67**: 7399–7409.
- Park, S.R., Paik, J.H., Ahn, M.S., Park, J.W., and Yoon, Y.J. (2010) Biosynthesis of plant-specific flavones and flavonols in *Streptomyces venezuelae*. *J Microbiol Biotechnol* **20**: 1295–1299.
- Park, S.R., Yoon, J.A., Paik, J.H., Park, J.W., Jung, W.S., Ban, Y.-H., *et al.* (2009) Engineering of plant-specific

- phenylpropanoids biosynthesis in *Streptomyces venezuelae*. *J Biotechnol* **141**: 181–188.
- Pelissero, C., Lenczowski, M.J.P., Chinzi, D., Davail-Cuisset, B., Sumpter, J.P., and Fostier, A. (1996) Effects of flavonoids on aromatase activity, an in vitro study. *J Steroid Biochem Mol Biol* **57**: 215–223.
- Prescott, A.G., Stamford, N.P.J., Wheeler, G., and Firmin, J.L. (2002) In vitro properties of a recombinant flavonol synthase from *Arabidopsis thaliana*. *Phytochemistry* **60**: 589–593.
- Ravishankar, D., Rajora, A.K., Greco, F., and Osborn, H.M.I. (2013) Flavonoids as prospective compounds for anti-cancer therapy. *Int J Biochem Cell Biol* **45**: 2821–2831.
- Redondo-Blanco, S., Fernández, J., Gutiérrez-del-Río, I., Villar, C.J., and Lombó, F. (2017) New insights toward colorectal cancer chemotherapy using natural bioactive compounds. *Front Pharmacol* **8**: 109.
- Rodríguez, A., Strucko, T., Stahlhut, S.G., Kristensen, M., Svenssen, D.K., Forster, J., et al. (2017) Metabolic engineering of yeast for fermentative production of flavonoids. *Bioresour Technol* **245**: 1645–1654.
- Rozmer, Z., and Perjési, P. (2016) Naturally occurring chalcones and their biological activities. *Phytochem Rev* **15**: 87–120.
- Sambrook, J., and Russell, D.W. (2001) *Molecular Cloning: A Laboratory Manual*. Cold Spring Harbor, NY: CSHL Press.
- Sánchez, M., Romero, M., Gómez-Guzmán, M., Tamargo, J., Pérez-Vizcaino, F., and Duarte, J. (2019) Cardiovascular effects of flavonoids. *Curr Med Chem* **26**: 6991–7034.
- Santos, C.N.S., Koffas, M., and Stephanopoulos, G. (2011) Optimization of a heterologous pathway for the production of flavonoids from glucose. *Metab Eng* **13**: 392–400.
- Shah, F.L.A., Ramzi, A.B., Baharum, S.N., Noor, N.M., Goh, H.-H., Leow, T.C., et al. (2019) Recent advancement of engineering microbial hosts for the biotechnological production of flavonoids. *Mol Biol Rep* **46**: 6647–6659.
- Shen, X., Martens, S., Chen, M., Li, D., Dong, J., and Wang, T. (2010) Cloning and characterization of a functional flavanone-3 β -hydroxylase gene from *Medicago truncatula*. *Mol Biol Rep* **37**: 3283–3289.
- Stahlhut, S.G., Siedler, S., Malla, S., Harrison, S.J., Maury, J., Neves, A.R., and Forster, J. (2015) Assembly of a novel biosynthetic pathway for production of the plant flavonoid fisetin in *Escherichia coli*. *Metab Eng* **31**: 84–93.
- Stevens, J.F., Ivancic, M., Deinzer, M.L., and Wollenweber, E. (1999) A Novel 2-Hydroxyflavanone from *Collinsonia canadensis*. *J Nat Prod* **62**: 392–394.
- Sun, Y.-J., He, J.-M., and Kong, J.-Q. (2019) Characterization of two flavonol synthases with iron-independent flavanone 3-hydroxylase activity from *Ornithogalum caudatum* Jacq. *BMC Plant Biol* **19**: 195.
- Ta, N., and Walle, T. (2007) Aromatase inhibition by bioavailable methylated flavones. *J Steroid Biochem Mol Biol* **107**: 127–129.
- Takamura, Y., and Nomura, G. (1988) Changes in the intracellular concentration of Acetyl-CoA and Malonyl-CoA in relation to the carbon and energy metabolism of *Escherichia coli* K12. *Microbiology* **134**: 2249–2253.
- Takano, H., Matsui, Y., Nomura, J., Fujimoto, M., Katsumata, N., Koyama, T., et al. (2017) High production of a class III lantipeptide AmfS in *Streptomyces griseus*. *Biosci Biotechnol Biochem* **81**: 153–164.
- Ti, H., Wu, P., Lin, L., and Wei, X. (2011) Stilbenes and flavonoids from *Artocarpus nitidus* subsp. *lingnanensis*. *Fitoterapia* **82**: 662–665.
- Trantas, E.A., Koffas, M.A.G., Xu, P., and Ververidis, F. (2015) When plants produce not enough or at all: metabolic engineering of flavonoids in microbial hosts. *Front Plant Sci* **6**: 1–16.
- Tsao, R. (2010) Chemistry and biochemistry of dietary polyphenols. *Nutrients* **2**: 1231–1246.
- Verdel-Aranda, K., López-Cortina, S.T., Hodgson, D.A., and Barona-Gómez, F. (2015) Molecular annotation of ketol-acid reductoisomerases from *Streptomyces* reveals a novel amino acid biosynthesis interlock mediated by enzyme promiscuity. *Microb Biotechnol* **8**: 239–252.
- Verma, A.K., and Pratap, R. (2010) The biological potential of flavones. *Nat Prod Rep* **27**: 1571–1593.
- Wang, T., Bai, L., Zhu, D., Lei, X., Liu, G., Deng, Z., and You, D. (2012) Enhancing macrolide production in *Streptomyces* by coexpressing three heterologous genes. *Enzyme Microb Technol* **50**: 5–9.
- Wang, Y., Chen, S., and Yu, O. (2011) Metabolic engineering of flavonoids in plants and microorganisms. *Appl Microbiol Biotechnol* **91**: 949–956.
- Watts, K.T., Lee, P.C., and Schmidt-Dannert, C. (2004) Exploring recombinant flavonoid biosynthesis in metabolically engineered *Escherichia coli*. *ChemBioChem* **5**: 500–507.
- Wellmann, F., Matern, U., and Lukačín, R. (2004) Significance of C-terminal sequence elements for *Petunia* flavanone 3 β -hydroxylase activity. *FEBS Lett* **561**: 149–154.
- Wu, J., Wang, X.-C., Liu, Y., Du, H., Shu, Q.-Y., Su, S., et al. (2016) Flavone synthases from *Lonicera japonica* and *L. macranthoides* reveal differential flavone accumulation. *Sci Rep* **6**: 19245.
- Xue, Z., McCluskey, M., Cantera, K., Sariaslani, F.S., and Huang, L. (2007) Identification, characterization and functional expression of a tyrosine ammonia-lyase and its mutants from the photosynthetic bacterium *Rhodobacter sphaeroides*. *J Ind Microbiol Biotechnol* **34**: 599–604.
- Yang, W.Z., Ye, M., Qiao, X., Wang, Q., Bo, T., & Guo, D.A. (2012) Collision-induced dissociation of 40 flavonoid aglycones and differentiation of the common flavonoid subtypes using electrospray ionization ion-trap tandem mass spectrometry and quadrupole time-of-flight mass spectrometry. *Eur J Mass Spectrom* **18**: 493–503.
- Yao, B., Fang, H., Xu, W., Yan, Y., Xu, H., Liu, Y., et al. (2014) Dietary fiber intake and risk of type 2 diabetes: A dose-response analysis of prospective studies. *Eur J Epidemiol* **29**: 79–88.
- Yonekura-Sakakibara, K., Higashi, Y., and Nakabayashi, R. (2019) The origin and evolution of plant flavonoid metabolism. *Front Plant Sci* **10**: 943.
- Yu, Q., Zeng, K., Ma, X., Song, F., Jiang, Y., Tu, P., and Wang, X. (2016) Resokaempferol-mediated anti-inflammatory effects on activated macrophages via the inhibition of JAK2/STAT3, NF- κ B and JNK/p38 MAPK signaling pathways. *Int Immunopharmacol* **38**: 104–114.

Zhang, J., Subramanian, S., Zhang, Y., and Yu, O. (2007) Flavone synthases from *Medicago truncatula* are Flavanone-2-hydroxylases and are important for nodulation. *Plant Physiol* **144**: 741–751.

Supporting information

Additional supporting information may be found online in the Supporting Information section at the end of the article.

Fig. S1. MS spectra (first column), MS² spectra for the parent ion m/z 271.0535 [M-H]⁻ (second column) and MS² spectra for the in-source-formed species m/z 243.0591 [M-H]⁻ (third column). A-C, MS and MS² spectra of purified 2-hydroxyliquiritigenin. In B, daughter ions m/z 253.0461 and m/z 209.0554 were also detected but are not visible due to the scale; D-F, MS and MS² spectra of authentic garbanzol; and G-H, MS and MS² spectra of authentic butin.

Fig. S2. Overlaid EICs for several flavonoids, *p*-coumaric acid and chalcone liquiritigenin of *S. albus* pGR (B) and *S. albus* pDF crude extracts (C) compared with commercial standards (A). X-axis has been zoomed at 3.5–8 min. Y-axis has been modified to clearly show all peaks; hence, peak intensities cannot be compared. *p*COU, *p*-coumaric acid (two peaks were detected, representing *cis-p*-coumaric acid and *trans-p*-coumaric acid); DHK, dihydrokaempferol; 7,4'-DHF, 7,4'-dihydroxyflavone; LIQ, liquiritigenin; ILQ,

isoliquiritigenin; RSK, resokaempferol; 2OH-NAR; 2-hydroxynaringenin; API, apigenin; NRG, naringenin; KAE, kaempferol; ERI, eriodictyol; 2OH-LIQ, 2-hydroxyliquiritigenin (no commercial standard available); FUS, fustin; QRC, quercetin; DHQ, dihydroquercetin; GRB, garbanzol.

Fig. S3. Production titres in $\mu\text{g l}^{-1}$ of several flavonoids, chalcone isoliquiritigenin and *p*-coumaric acid in recombinant *S. albus* pGR and *S. albus* pDF strains as well as in *S. albus* pAGO-negative control strain. *: 7,4'-DHF was detected in *S. albus* pGR, *S. albus* pDF and *S. albus* pGR + 0.1 mM NRG but in LOQ (limit of quantification), as well as 2OH-NRG and RSK in *S. albus* pGR + 0.1 mM NRG. The mean value of compounds was calculated from three biological replicates. *p*COU, *p*-coumaric acid; DHK, dihydrokaempferol; 7,4'-DHF, 7,4'-dihydroxyflavone; LIQ, liquiritigenin; ILQ, isoliquiritigenin; RSK, resokaempferol; 2OH-NAR; 2-hydroxynaringenin; API, apigenin; NRG, naringenin; KAE, kaempferol; FUS, fustin; QRC, quercetin; DHQ, dihydroquercetin; GRB, garbanzol.

Fig. S4. Comparison of main flavonoid intermediates as seen in the extracted supernatant (A) and cellular pellet (B) in *S. albus* pGR (overlaid EICs from HPLC-MS data). Same extracts concentrations were injected in the HPLC-MS equipment.

Fig. S5. EICs at m/z 271.06118 \pm 0.005 [M-H]⁻ of *S. albus* pGR crude extract sampled every 24 h over 168 h. The scale of the Y-axis is fixed to the highest intensity value at 144 h.

Appendix S1. Supplementary material.